



Observation of Photons above 300 TeV Associated with a High-energy Neutrino from the Cygnus Region

D. D. Dzhappuev¹, Yu. Z. Afashokov¹, I. M. Dzaparova^{1,2}, T. A. Dzhatdoev^{1,3}, E. A. Gorbacheva¹, I. S. Karpikov¹, M. M. Khadzhiev¹, N. F. Klimenko¹, A. U. Kudzhaev¹, A. N. Kurenya¹, A. S. Lidvansky¹, O. I. Mikhailova¹, V. B. Petkov^{1,2}, E. I. Podlesnyi^{1,3,4}, V. S. Romanenko¹, G. I. Rubtsov¹, S. V. Troitsky¹, I. B. Unatlov¹, I. A. Vaiman^{3,4}, A. F. Yanin¹, Ya. V. Zhezher^{1,5}, and K. V. Zhuravleva¹,
(Carpet–3 Group)

¹Institute for Nuclear Research of the Russian Academy of Sciences, 60th October Anniversary Prospect 7a, Moscow 117312, Russia; st@ms2.inr.ac.ru

²Institute of Astronomy, Russian Academy of Sciences, 119017, Moscow, Russia

³D.V. Skobel'tsyn Institute of Nuclear Physics, M.V. Lomonosov Moscow State University, Moscow 119991, Russia

⁴Physics Department, M.V. Lomonosov Moscow State University, Moscow 119991, Russia

⁵Institute for Cosmic Ray Research, University of Tokyo, Kashiwa, Kashiwanoha, 5-1-5, 277-8582, Japan

Received 2021 May 15; revised 2021 July 3; accepted 2021 July 15; published 2021 August 4

Abstract

Galactic sites of acceleration of cosmic rays to energies of order 10^{15} eV and higher, dubbed PeVatrons, reveal themselves by recently discovered gamma radiation of energies above 100 TeV. However, joint gamma-ray and neutrino production, which marks unambiguously cosmic-ray interactions with ambient matter and radiation, was not observed until now. In 2020 November, the IceCube neutrino observatory reported an ~ 150 TeV neutrino event from the direction of one of the most promising Galactic PeVatrons, the Cygnus Cocoon. Here we report on the observation of a 3.1σ (post-trial) excess of atmospheric air showers from the same direction, observed by the Carpet–2 experiment and consistent with a few months flare in photons above 300 TeV, in temporal coincidence with the neutrino event. The fluence of the gamma-ray flare is of the same order as that expected from the neutrino observation, assuming the standard mechanism of neutrino production. This is the first evidence for the joint production of high-energy neutrinos and gamma-rays in a Galactic source.

Unified Astronomy Thesaurus concepts: [Neutrino astronomy \(1100\)](#); [Gamma-rays \(637\)](#)

1. Introduction

Recent observations of astrophysical gamma-rays above 100 TeV established the existence of various Galactic sources, both point-like (Abeysekara et al. 2019, 2020; Amenomori et al. 2019; Albert et al. 2020, 2021; Cao et al. 2021) and diffuse (Amenomori et al. 2021). These observations are often interpreted as indications to the existence of Galactic PeVatrons, that are sites of cosmic-ray acceleration up to \gtrsim PeV energies,⁶ in which the gamma-rays are produced in interactions of energetic hadrons with ambient matter and radiation. Observations of neutrinos co-produced with these gamma-rays would unambiguously point to their hadronic origin.

Whether or not some of the high-energy (above TeV) astrophysical neutrinos (Aartsen et al. 2013a, 2013b; for recent reviews, see, e.g., Ahlers & Halzen 2018; Palladino et al. 2020) come from Galactic sources is an intriguing question. While the largest available data set of the IceCube and ANTARES experiments does not demonstrate any correlation of neutrino arrival directions with the Galactic disk (Albert et al. 2018), various indications exist in favor of the Galactic origin of a part of the neutrino flux at energies below ~ 200 TeV. The most recent analysis of arrival directions of IceCube cascade events (Aartsen et al. 2019) reveals a weak Galactic-plane excess. Studies of track-like and cascade-like events registered in the IceCube detector under the assumption of the power-law shape of the primary neutrino spectrum yield (e.g., Abbasi et al. 2021) different values of the power-law index for these two samples of events. This

discrepancy may be explained naturally if the primary spectrum is actually composed of two distinct components (Chen et al. 2015). A population of extragalactic sources that demonstrates a significant correlation with astrophysical neutrinos (Plavin et al. 2021) may be responsible for the hard component, while the soft component may be due to the Galactic sources (Palladino et al. 2016; Palladino & Vissani 2016). In the latter case, the extragalactic gamma-ray background (EGRB) component concomitant with IceCube neutrinos does not overshoot the EGRB measured with Fermi-LAT.

Cygnus Cocoon (Ackermann et al. 2011), an extended gamma-ray source presumably containing an OB star association embedded in a super-bubble, is a candidate Galactic hadronic PeVatron. Star-forming regions are potential sites of cosmic-ray acceleration, and gamma-ray and neutrino production (Bykov et al. 2020). In particular, it has been predicted that the flux of high-energy neutrinos from Cygnus Cocoon is close to the IceCube sensitivity (Yoast-Hull et al. 2017). This source was detected by HAWC up to, and possibly beyond, 100 TeV (Abeysekara et al. 2020, 2021); its position is consistent with the highest-energy (up to 1.4 PeV) photon source detected by LHAASO (Cao et al. 2021). Gamma-ray sources in the Cygnus region contribute a lot to the Galactic-plane diffuse gamma radiation above 400 TeV, discovered by Amenomori et al. (2021).

On 2020 November 20, IceCube reported (IceCube Collaboration 2020) a candidate track-like neutrino event with the estimated energy of 154 TeV. The arrival direction of the neutrino, though determined with a considerably low precision, coincided with the direction from Cygnus Cocoon. The event

⁶ 1 PeV = 10^{15} eV.

was reported through the standard BRONZE alert procedure (Blaufuss et al. 2019). These alerts are followed up routinely by numerous instruments, in particular (Dzhappuev et al. 2020c) by the Carpet–2 gamma-ray telescope at the Baksan Neutrino Observatory. This event, however, was exceptional in the sense that it coincided with a previously defined prospective Galactic source of high-energy neutrinos. This provides an opportunity to detect sub-PeV gamma-rays co-produced with neutrinos, which cannot reach us from extragalactic sources because of pair production on cosmic microwave background radiation (Nikishov 1962). Standard Carpet–2 alert analysis revealed two gamma-ray candidate events in a one-month interval centered at the alert time (Dzhappuev et al. 2020a). Here, we present results of a more detailed study of a possible sub-PeV gamma-ray flare in the Cygnus Cocoon associated with the IceCube neutrino event.

2. The Carpet–2 Detector and the Data Set

Carpet–2 is an air-shower experiment co-located with the Baksan Neutrino Observatory (Neutrino village, North Caucasus). It includes a 200 m² continuous central scintillator detector, Carpet; five outer detector stations with 9 m² of scintillator in each of them; and a 175 m² shielded detector with the threshold of 1 GeV for vertical muons. The primary-particle energy is determined from the shower size N_e , reconstructed from the central Carpet; the arrival direction is obtained from timing of the outer stations; the muon detector is used to select candidate gamma-ray showers that are muon-poor. The installation, its operation, and data processing are described by Dzhappuev et al. (2007), Szabelski & Carpet–3 Collaboration (2009), Dzhappuev et al. (2016, 2019a), and Troitsky et al. (2019).

The angular resolution of Carpet–2 is determined by a combination of (i) fluctuations in the shower, (ii) fluctuations in electronics, and (iii) earlier trigger of individual detector station due to coincident atmospheric muons. The point-spread function (PSF) has been determined experimentally (Alexeenko et al. 2003) by means of simultaneous observations of air showers by Carpet and by an atmospheric Cherenkov detector (CD). The pointing accuracy of the CD, 0^o.1, and its angular resolution, 0^o.6, have been measured from observations of bright stars. The PSF of Carpet is non-Gaussian; 86% of events are reconstructed within 4^o.7 of their true direction. Monte Carlo simulations and experimental measurements of individual contributions (i), (ii), and (iii) give results consistent with this estimate.

For the present study, we use Carpet–2 data recorded between 2018 April 7 and 2021 April 25, a total of 829 days of data collection. Standard quality cuts require that ≥ 500 GeV air-shower energy is deposited in Carpet; four outer stations participate in the determination of the arrival direction; the reconstructed shower axis is at least 0.7 m within the Carpet boundary; the reconstructed zenith angle is $\leq 40^\circ$. In total, 65,703 events passed these cuts in this time period.

3. Simulations and Data Analysis

Monte Carlo simulations that we use include air-shower modeling and the detector-response simulation described by Dzhappuev et al. (2019b). Every simulated event is recorded in the same format and reconstructed by the same program as those used for the real data, including the quality-cut selection. These simulations are used to relate the reconstructed shower

size N_e to the primary gamma-ray energy E_γ , to estimate the detection and reconstruction efficiency and to develop criteria for separation between events induced by primary photons and by cosmic rays. Because the efficiency of the detection of gamma-ray events drops quickly below $E_\gamma \sim 300$ TeV (Troitsky et al. 2019), we include only 56,969 events with reconstructed $E_\gamma > 300$ TeV in the data sample we use here. The effective area of the installation as the function of energy is presented by Dzhappuev et al. (2020c). Carpet–2 tests the same range of energies and fluxes for gamma-rays as IceCube tests for neutrinos.

We also determine the notion of a “photon median candidate event” (Abraham et al. 2008) from simulations as follows. Assuming the E_γ^{-2} primary spectrum, we simulate a large number of gamma-ray-induced events and select those with reconstructed $E_\gamma > 300$ TeV. For each of those events, we calculate the ratio of the number of muons in the shielded detector, n_μ , to N_e and select the value α such that 50% of reconstructed gamma-rays satisfy $n_\mu/N_e < \alpha$. In the search for gamma-ray flares of localized sources, when the isotropic and uniform in time cosmic-ray background is small, it makes sense to use also the directional and temporal coincidence as a distinctive criterion for primary photons: cosmic-ray particles are charged and, at the sub-PeV energies that we study here, isotropized in their directions and smeared in arrival times by the Galactic magnetic field. In this work, we use the entire sample to search for the gamma-ray excess associated with the neutrino event, then repeat the same procedure for the events selected by the “photon median” cut and check that the results are consistent. In this way, we both increase the available statistics and make the study less sensitive to the assumption about the source gamma-ray spectrum.

Previous Monte Carlo simulations for this (Alexeenko et al. 2003) and other (Gorbunov et al. 2006) air-shower experiments indicated that counting of events within the (86–90)% PSF containment angle is optimal in terms of the signal-to-noise ratio for point-source searches. In what follows, we concentrate on the circular region in the sky of this (86% PSF) 4^o.7 angular radius, centered at the fourth Fermi-LAT source catalog (4FGL; Abdollahi et al. 2020) best-fit position of the source 4FGL J2028.6+4110e, associated with the Cygnus Cocoon, and call this region the Cygnus–Cocoon Circle (CCC).

In the full 3 yr Carpet–2 data sets, defined above, the number of events in CCC is consistent with that expected from random background, so the source is not detected significantly above 300 TeV. We obtain an upper limit on its integral gamma-ray flux as $L_\gamma(E_\gamma > 300 \text{ TeV}) < 2.6 \times 10^{-13} \text{ cm}^{-2} \text{ s}^{-1}$ (95% CL). The situation is different when the time period around the neutrino event is considered.

To search for a flux enhancement around the neutrino event, we proceed as follows. Denote the total number of events observed from the CCC as N . As we have no prejudice about the possible flare time window, we consider the duration of the putative flare as a free parameter d and vary $d/2$ between 1 and 60 days around the neutrino event, in steps of 1 day. For each of these 60 time windows, we determine the number $M(d)$ of events from CCC in this period and calculate the binomial probability $p(d)$ to observe this or larger number of events assuming constant mean rate of events per day. We then find the pre-trial p -value $p_{\text{pre}} = \min_d p(d)$. To estimate the effect of multiple trials, we perform a Monte Carlo simulation of 10^4 mock sets of arrival times of N events. For each mock set i , we

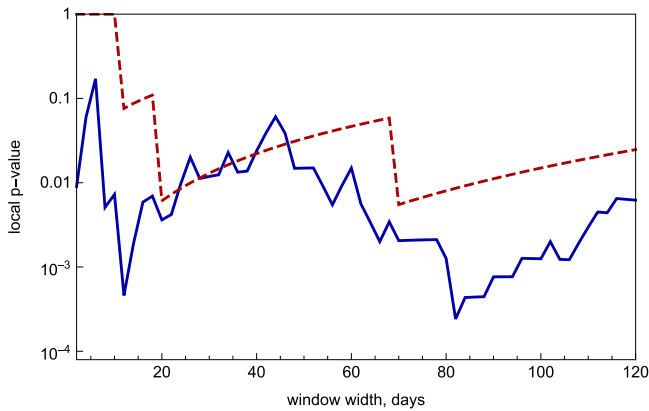


Figure 1. Dependence of the p -value on the width of the window centered on the neutrino arrival time (full line: all events, dashed line: photon median selection). See the text for details.

repeat the same procedure of varying the window width and finding the mock pre-trial p -value, p_i . The fraction of mock sets with $p_i \leq p_{\text{pre}}$ gives the post-trial probability p , which determines the significance of the observed effect, if any.

4. Results and Discussion

There are $N = 346$ events with arrival directions from CCC during 829 days of data collection, five of which are “photon median candidates”. Figure 1 presents the probability $p(d)$ for these two sets. For the full set, $p_{\text{pre}} = 2.4 \times 10^{-4}$ and is achieved for $d = 82$ (we note, however, that $p(d = 12)$ is almost that low). Stated in Gaussian terms, this value of p_{pre} would correspond to the 3.67σ (pre-trial) significance of the flare at the neutrino arrival time. However, the correction for window-width trials reduces the significance to $p = 1.5 \times 10^{-3}$ (3.17σ post-trial). The results for photon median candidate selection alone are $p_{\text{pre}} = 5.5 \times 10^{-3}$ (2.78σ pre-trial), optimal $d = 70$ and $p = 1.1 \times 10^{-2}$ (2.55σ post-trial). Figure 2 presents the number of events in a sliding window of the width $d = 82$ days of data collection centered at a certain date, as a function of this date. One can clearly see the enhancement around the neutrino event, consistent between all events and photon median candidates.

While the strongest signal was found for a flare with the duration of 82 days of data collection (85 calendar days), this particular number may be altered by fluctuations. The number of excess events is obtained from the time window that is tuned to have the strongest signal, so it may also be biased. The time-window correction that eliminates the effect of the flare duration tuning is applied, and the photon-flare parameters are estimated by Monte Carlo simulations; see the Appendix. We obtain the flare duration of $89.5^{+32.0}_{-18.6}$ days and the source flux during this flare of $I_\gamma(E_\gamma > 300 \text{ TeV}) = (5.6 \pm 1.8) \times 10^{-12} \text{ cm}^{-2} \text{ s}^{-1}$. We also define the fluence as the flux time-integrated over the flare, $13 \pm 4 \text{ GeV cm}^{-2}$.

It is instructive to compare this fluence in $E_\gamma > 300 \text{ TeV}$ photons with an estimate of the fluence of the putative neutrino flare. IceCube did not find a statistically significant excess of low-energy neutrinos associated with the alert on a day scale (Pizzuto & IceCube Collaboration 2020), nor additional high-energy neutrino alerts from this direction were reported, so the rough estimate of the neutrino fluence is determined by the single alert event (IceCube Collaboration 2020) and, given

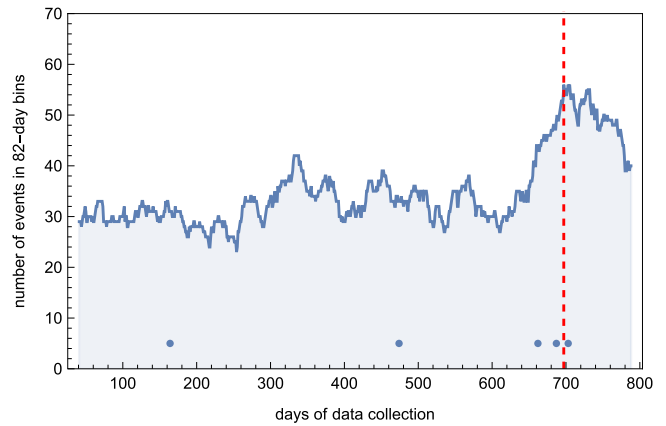


Figure 2. Number of events in $d = 82$ days bins centered at a given day of data collection. Dots indicate the days of arrival of photon median candidate events. The vertical dashed line indicates the neutrino arrival time.

the IceCube effective area for the BRONZE alert selection (Blaufuss et al. 2019), is of order $\sim 3.5 \text{ GeV cm}^{-2}$ (Dzhappuev et al. 2020a).⁷ Therefore, the orders of magnitude of the observed fluences are consistent with each other: in the standard pi-meson neutrino production mechanism, the energy in gamma-rays is about twice the energy in neutrinos.

Small statistics and large background make it unfeasible to derive the observed gamma-ray spectrum above 300 TeV. However, we note that a comparison of the numbers of excess of events in the full data set and among the photon median candidates speaks in favor of a hard spectrum: the excess in the former is larger than twice the excess in the latter. For instance, for a very hard $E_\gamma^{-1.4}$ spectrum, only one-third of photons pass the median cut designed assuming the E_γ^{-2} spectrum that we use. Such hard spectra do not look implausible in view of recent theoretical (Bykov et al. 2018) and observational (Dzhatdov et al. 2021) results. Additionally, we reconstructed the spectral energy distribution (SED; $\text{SED} \equiv E^2 dN/dE \equiv E^2 F_\gamma$) of Cygnus Cocoon in the energy range from 100 MeV to 1 TeV averaged over the same $d = 82$ days period around the neutrino arrival using publicly available data of the Fermi Large Area Telescope (Fermi-LAT) (Atwood et al. 2009). The region of interest (ROI) in our analysis was a 15° square centered at the 4FGL position of the Cygnus Cocoon. Making use of *fermitools*⁸ (version 2.0.8) and *fermipy* (version 1.0.1; Wood et al. 2017) packages and the instrument response function P8R3_SOURCE_V3, we constructed a model of the observed gamma-ray emission from the region of interest (ROI) containing 4FGL sources, including our source of interest 4FGL J2028.6+4110e; models of the isotropic gamma-ray background `iso_P8R3_SOURCE_V3_v1` and the galactic diffuse emission `gll_iem_v07`. Normalizations of both diffuse backgrounds and the spectral shape of the galactic diffuse emission, along with all spectral parameters of the source of interest, were left free. The normalizations for other sources within 5° from the ROI center were also left free, but their spectral shapes and all parameters of sources beyond the 5° circle were fixed to the catalog values. Other event selection parameters were set according to the standard recommendations of the Fermi-LAT collaboration

⁷ This gives an order-of-magnitude estimate only because of the Eddington bias in the flux estimation of a single event, cf. Strotjohann et al. (2019), large uncertainties in the energy estimation of track events and the lack of information about neutrino events in the days around the alert.

⁸ <https://github.com/fermi-lat/Fermitools-conda>

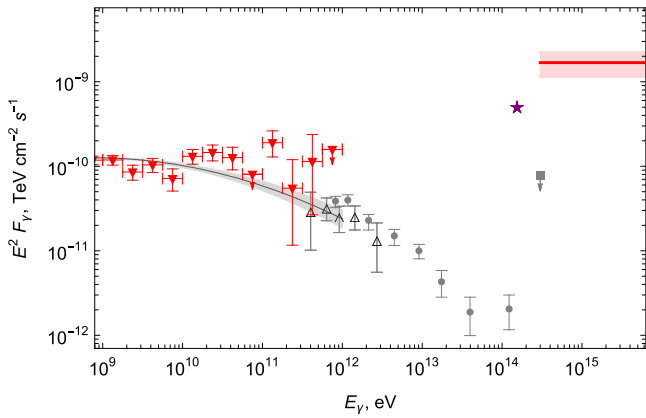


Figure 3. Spectral energy distribution (SED) of Cygnus Cocoon above 1 GeV. Gray color: time-averaged (line, 4FGL flux model (Abdollahi et al. 2020)); open triangles, ARGO (Bartoli et al. 2014); circles, HAWC (Abeysekara et al. 2021); box, Carpet-2, this work). Red color: flare (triangles, Fermi-LAT; line, Carpet-2—this work). Purple star: estimate of the neutrino fluence. See the text for details.

for a galactic point-source analysis.⁹ Using `GTAnalysis.sed_fermipy` method we obtained the SED of 4FGL J2028.6+4110e averaged over the 82 days flare period. We found an indication ($\sim 2.17\sigma$ significance) of the spectrum hardening with respect to the spectrum of the Cygnus Cocoon presented in the 4FGL catalog.

Figure 3 compares our observations with other high-energy data. Unfortunately, no simultaneous data on the month-scale flare related to the neutrino arrival have yet been published by other experiments.

The source entered the field of view of Carpet-2 16 minutes after the neutrino arrival. Like HAWC (Ayala & HAWC Collaboration 2020), we do not find a significant flux enhancement within 24 hr from the neutrino (Dzhappuev et al. 2020b). However, we observed a very unusual cluster of events at the scale of minutes on the day of the neutrino alert; its significance and implications will be discussed elsewhere.

5. Conclusions

An excess of events was observed by Carpet-2 from the direction of the Cygnus region in temporal coincidence with the IceCube neutrino alert from the same direction. Statistical significance of the excess is 3.1σ post-trial. The excess may be interpreted as a $E_\gamma > 300$ TeV photon flare with the duration of ~ 3 months around the neutrino event and the fluence of 13 ± 4 GeV cm⁻². For the first time, rare sub-PeV neutrino and gamma-rays from the direction of a prospective Galactic PeVatron were observed in directional and temporal coincidence. This observation supports previously proposed scenarios of the origin of a part of observed high-energy neutrinos in pi-meson decays in Galactic sources. Note that poor localization of the neutrino event, as well as the modest angular resolution of Carpet-2, leave open the possibility of the association of these events with other interesting sources in CCC, including the gamma-ray loud micro-quasar Cyg X-3, gamma-ray binary PSR J2032+4027 etc.

This possible sub-PeV flare may be searched in the recorded data of other gamma-ray air-shower experiments, LHAASO (Cao 2010), HAWC (Abeysekara et al. 2013), Tibet (Sako et al. 2009), GRAPES3 (Hayashi et al. 2005), and TAIGA

(Budnev et al. 2020), as well as of neutrino telescopes, IceCube (Aartsen et al. 2017) in the track mode and ANTARES (Ageron et al. 2011), and Baikal-GVD (Avrorin et al. 2011) in the cascade mode. Future monitoring of the source by these instruments, as well as by the upgraded Carpet-3 (Kudzaev et al. 2019), is also encouraged.

We thank A. Bykov, T.-Q. Huang, K. Kawata and D. Semikoz for illuminating discussions. This work is supported by the Ministry of science and higher education of Russian Federation under the contract 075-15-2020-778. E.I.P. thanks the Foundation for the Advancement of Theoretical Physics and Mathematics “BASIS” (Contract No. 20-2-10-7-1) and the Non-profit Foundation for the Advancement of Science and Education “Intellect” for the student scholarships.

Facilities: Carpet-2, IceCube neutrino observatory, Fermi-LAT.

Appendix

Estimation of the Flare Duration and Fluence





Estimation of the number of signal events—Assume that the flare flux corresponds to x photons during the flare period and the photon spectrum is E^{-2} . Of them, on average, we expect the excess of $x/2$ photon median candidates and $x/2$ other events above the background rates of $b_1 \approx 0.25$ for photon median candidates and $b_2 \approx 32.2$ for the rest of events (determined from the off-flare period of observations). We thus expect to observe $b_1 + x/2$ photon candidates and $b_2 + x/2$ other events during the flare, but all these numbers fluctuate. To determine x , we maximize the probability to observe the actual numbers of events, $o_1 = 3$ photon candidates and $o_2 = 53$ other events, simultaneously. We find $x \approx 9.9 \pm 3.2$; this number is divided by the effective exposure to determine the flux. Note that the probability to observe $\leq o_1$ and $\geq o_2$ events in the respective data sets is ≈ 0.07 for this x , so the two observations are consistent at the 93% CL.

Correction of the biases caused by trials—The flare window was chosen such that the excess is most significant. This procedure selects a positive fluctuation in the number of observed, signal plus background, events (the post-trial significance accounts for this). Thus this best duration of the flare and the corresponding excess flux are biased. To correct for this effect, we perform a Monte Carlo simulation of the entire procedure, assuming the flare parameters determined above. For each simulated realization of the events, we find the strongest signal flux and duration. Then we compare these reconstructed fluxes and durations with those assumed in the simulation. The reconstructed flux and duration differ from the true values by factors of 0.86 and 1.08, respectively. These coefficients are accounted for in the values reported in the main text.

ORCID iDs

D. D. Dzhappuev <https://orcid.org/0000-0001-9956-5439>
 Yu. Z. Afashokov <https://orcid.org/0000-0003-2652-0293>
 T. A. Dzhatdov <https://orcid.org/0000-0002-7660-4236>
 M. M. Khadzhiyev <https://orcid.org/0000-0002-0564-8477>
 N. F. Klimenko <https://orcid.org/0000-0003-4301-9599>
 A. U. Kudzaev <https://orcid.org/0000-0002-8337-3878>
 A. S. Lidvansky <https://orcid.org/0000-0002-8002-6491>
 O. I. Mikhailova <https://orcid.org/0000-0001-6146-8318>
 E. I. Podlesnyi <https://orcid.org/0000-0003-3395-0419>
 V. S. Romanenko <https://orcid.org/0000-0001-9784-2244>
 G. I. Rubtsov <https://orcid.org/0000-0002-6106-2673>

⁹ https://fermi.gsfc.nasa.gov/ssc/data/analysis/documentation/Cicerone/Cicerone_Data_Exploration/Data_preparation.html

S. V. Troitsky  <https://orcid.org/0000-0001-6917-6600>
 I. A. Vaiman  <https://orcid.org/0000-0002-8255-3631>
 Ya. V. Zhezher  <https://orcid.org/0000-0002-3588-9706>
 K. V. Zhuravleva  <https://orcid.org/0000-0001-6086-4247>

References

- Aartsen, M. G., Abbasi, R., Abdou, Y., et al. 2013a, *PhRvL*, **111**, 021103
 Aartsen, M. G., Ackermann, M., Adams, J., et al. 2013b, *Sci*, **342**, 1242856
 Aartsen, M. G., Ackermann, M., Adams, J., et al. 2017, *JINST*, **12**, P03012
 Aartsen, M. G., Ackermann, M., Adams, J., et al. 2019, *ApJ*, **886**, 12
 Abbasi, R., Ackermann, M., Adams, J., et al. 2021, *PhRvD*, **104**, 022002
 Abdollahi, S., Acero, F., Ackermann, M., et al. 2020, *ApJS*, **247**, 33
 Abeyssekara, A. U., Albert, A., Alfaro, R., et al. 2019, *ApJ*, **881**, 134
 Abeyssekara, A. U., Albert, A., Alfaro, R., et al. 2020, *PhRvL*, **124**, 021102
 Abeyssekara, A. U., Albert, A., Alfaro, R., et al. 2021, *NatAs*, **5**, 465
 Abeyssekara, A. U., Alfaro, R., Alvarez, C., et al. 2013, *Aph*, **50**, 26
 Abraham, J., Abreu, P., Aglietta, M., et al. 2008, *Aph*, **29**, 243
 Ackermann, M., Ajello, M., Allafort, A., et al. 2011, *Sci*, **334**, 1103
 Ageron, M., Aguilar, J. A., Al Samarai, I., et al. 2011, *NIM A*, **656**, 11
 Ahlers, M., & Halzen, F. 2018, *PPNP*, **102**, 73
 Albert, A., Alfaro, R., Alvarez, C., et al. 2020, *ApJL*, **896**, L29
 Albert, A., André, M., Anghinolfi, M., et al. 2018, *ApJL*, **868**, L20
 Albert, A., Alfaro, R., Alvarez, C., et al. 2021, *ApJL*, **907**, L30
 Alexeenko, V. V., Bakatanov, V. N., Dzhappuev, D. D., et al. 2003, “Carpet” installation: estimate of the angular resolution with a Cherenkov radiation detector, INR RAS Tech. Rep. 1109
 Amenomori, M., Bao, Y. W., Bi, X. J., et al. 2021, *PhRvL*, **126**, 141101
 Amenomori, M., Bao, Y. W., Bi, X. J., et al. 2019, *PhRvL*, **123**, 051101
 Atwood, W. B., Abdo, A. A., Ackermann, M., et al. 2009, *ApJ*, **697**, 1071
 Avrorin, A., Aynutdinov, V., Belolaptikov, I., et al. 2011, *NIMPA*, **639**, 30
 Ayala, H. & HAWC Collaboration 2020, GCN, **28952**, 1
 Bartoli, B., Bernardini, P., Bi, X. J., et al. 2014, *ApJ*, **790**, 152
 Blaufuss, E., Kintscher, T., Lu, L., & Tung, C. F. 2019, Proc. ICRC (Madison, WI), **36**, 1021
 Budnev, N., Astapov, I., Bezyazeev, P., et al. 2020, *JINST*, **15**, C09031
 Bykov, A. M., Ellison, D. C., Gladilin, P. E., & Osipov, S. M. 2018, *AdSpR*, **62**, 2764
 Bykov, A. M., Marcowith, A., Amato, E., et al. 2020, *SSRv*, **216**, 42
 Cao, Z. 2010, *ChPhy*, **34**, 249
 Cao, Z., Aharonian, F. A., An, Q., et al. 2021, *Natur*, **594**, 33
 Chen, C.-Y., Bhupal Dev, P. S., & Soni, A. 2015, *PhRvD*, **92**, 073001
 Dzhappuev, D., Kudzhaev, A., Petkov, V., & Troitsky, S. 2020a, *ATeL*, **14255**, 1
 Dzhappuev, D., Kudzhaev, A., Petkov, V., & Troitsky, S. 2020b, *ATeL*, **14237**, 1
 Dzhappuev, D. D., Afashokov, Y. Z., Dzaparova, I. M., et al. 2020c, *JETPL*, **112**, 753
 Dzhappuev, D. D., Alekseenko, V. V., Volchenko, V. I., et al. 2007, *BRASP*, **71**, 525
 Dzhappuev, D. D., Dzaparova, I. M., Gorbacheva, E. A., et al. 2019a, *EPJWC*, **207**, 03004
 Dzhappuev, D. D., Dzaparova, I. M., Gorbacheva, E. A., et al. 2019b, *JETPL*, **109**, 226
 Dzhappuev, D. D., Petkov, V. B., Kudzhaev, A. U., et al. 2016, in SAO RAS Conf. Proc. Quark Phase Transition in Compact Objects and Multimessenger Astronomy: Neutrino Signals, Supernovae and Gamma-Ray Bursts, ed. V. V. Sokolov et al. (Pyatigorsk: Sneg), **30**
 Dzhathoev, T., Podlesnyi, E., & Vaiman, I. 2021, arXiv:2101.10781
 Gorbunov, D. S., Tinyakov, P. G., Tkachev, I. I., & Troitsky, S. V. 2006, *JCAP*, **01**, 025
 Hayashi, Y., Aikawa, Y., Gopalakrishnan, N. V., et al. 2005, *NIMPA*, **545**, 643
 IceCube Collaboration 2020, GCN, **28927**, 1
 Kudzhaev, A. U., Dzhappuev, D. D., Afashokov, Yu. Z., et al. 2019, *JPhCS*, **1390**, 012129
 Nikishov, A. I. 1962, *JETP*, **14**, 393
 Palladino, A., Spurio, M., & Vissani, F. 2016, *JCAP*, **12**, 045
 Palladino, A., Spurio, M., & Vissani, F. 2020, *Univ*, **6**, 30
 Palladino, A., & Vissani, F. 2016, *ApJ*, **826**, 185
 Pizzuto, A. & IceCube Collaboration 2020, GCN, **28946**, 1
 Plavin, A. V., Kovalev, Y. Y., Kovalev, Y. A., & Troitsky, S. V. 2021, *ApJ*, **908**, 157
 Sako, T. K., Kawata, K., Ohnishi, M., et al. 2009, *Aph*, **32**, 177
 Strotjohann, N. L., Kowalski, M., & Franckowiak, A. 2019, *A&A*, **622**, L9
 Szabelski, J. & Carpet-3 Collaboration 2009, *NuPhS*, **196**, 371
 Troitsky, S., Dzhappuev, D., & Zhezher, Y. 2019, Proc. ICRC (Madison, WI), **36**, 808
 Wood, M., Caputo, R., Charles, E., et al. 2017, Fermipy: An open-source Python package for analysis of Fermi-LAT Data, arXiv:1707.09551
 Yoast-Hull, T. M., Gallagher, J. S., Halzen, F., Kheirandish, A., & Zweibel, E. G. 2017, *PhRvD*, **96**, 043011